Exterior Surface Temperature and Humidity of Walls—Comparison of Experiment and Numerical Simulation

Andreas Holm, Dr.-Ing.
Associate Member ASHRAE

Wolfgang Zillig

Hartwig M. Künzel, Dr.-Ing.
Member ASHRAE

ABSTRACT

The conditions at the exterior surface of building components with high insulation are almost independent of the indoor climate. The tiny heat flow from the interior is generally not sufficient to prevent a temperature drop below ambient conditions by long-wave emission during nighttime. Apart from energetic consequences, this temperature drop may lead to surface condensation and subsequently to soiling or microbial growth. Another factor resulting in surface temperatures below ambient conditions is the evaporation of precipitation moisture.

In order to obtain realistic surface conditions by numerical simulation, the heat and moisture transfer processes at the surface have to be modeled accurately, taking into account convective and radiative exchange as well as evaporation and condensation heat. This requires hourly climatic data including air temperature and humidity, solar and sky radiation, precipitation, wind speed and direction. These data from selected years recorded at the meteorological station of the Fraunhofer-IBP in Holzkirchen serve as input for a hygrothermal simulation tool called WUFI®. The calculated results are compared with measured surface temperatures of walls and roofs with different orientation at the Fraunhofer-IBP test site. From this comparison appropriate surface transfer coefficients for simulation tools can be deduced and the different surface humidity sources may be quantified.

INTRODUCTION

In recent years problems with algae growth on façades (Klinkenberg and Venzmer 2000; Künzel and Sedbauer 2001) have been reported that are linked to nighttime condensation on the exterior surface due to radiative cooling of the façade. To solve the algae problem and save energy at the same time, low infrared emissivity coatings have been developed and tested (Leonhardt and Sinnesbichler 2000). Another problem caused by nighttime overcooling is the moisture uptake of vented attics or cathedral ceilings due to the condensation of outdoor air humidity in the ventilated spaces (Künzel and Groβkinsky1989; Hens 1990). All of these problems have been studied by field tests. Since experimental results are not easily transferable to other climatic regions or modified building assemblies, calculation tools simulating the real surface exchange processes are urgently required. However, most of the currently available calculation tools do not account for the different convective and radiative heat transfer processes at the exterior surface separately. They use lumped film coefficients and hence cannot predict nighttime overcooling in a correct way. Therefore, the PC software WUFI® (Künzel and Sedbauer 2001) has been modified to allow for a more detailed treatment of the thermal surface exchange. It also simplifies the calculation of moisture transfer at the surface that is connected to convective heat transfer only. The necessary equations of exchange, their implementation into WUFI® (Künzel 1995), and some example calculation results will be described in this paper.

In previous versions of WUFI®, which had originally been developed to simulate the hygrothermal processes within the material, long-wave radiation exchange of the façade with the surroundings was simply treated as an increase of the heat transfer coefficients. For most hygrothermal simulations, this simplified treatment is sufficient, since assessment of the

Andreas Holm is head of the Indoor Environmental and Climatic Impacts Department, **Wolfgang Zillig** is a researcher, and **Hartwig Künzel** is head of the Hygrothermal Department at Fraunhofer-IBP, Holzkirchen, Germany.

moisture balance in the construction usually does not require a perfectly detailed simulation of the thermal circumstances as long as the general temperature level is correctly reproduced. The situation changes for investigations that require more detailed treatment of the hygrothermal transfer aspects, such as an examination of nighttime surface temperatures or the study of surface heat and vapor fluxes and their dependence on ambient conditions or on the properties of the building envelope. These fluxes can depend very sensitively on details of the energy balance, and WUFI® has therefore been modified to meet these new requirements.

LONG-WAVE RADIATION EXCHANGE

In addition to solar radiation with an intensity peak at about 0.5 nm, a façade is also exposed to another distinct spectral range of radiation—long-wave radiation with a maximum intensity at about 10 nm. The facade itself emits long-wave radiation with an intensity that depends on its emissivity and its temperature ϑ:

$$E = 5.67 \cdot 10^{-8} \cdot \varepsilon \cdot (273 + \vartheta)^4$$

where

E = emitted long-wave energy flux (W/m²),

ε = emissivity (-),

ϑ = surface temperature (°C).

Nonmetallic surfaces usually have emissivities between approximately 0.8 and 1. Typical long-wave emissions are, therefore, roughly on the order of 300 W/m^2 at 0°C and 400 W/m^2 at 20°C.

On the other hand, the façade absorbs part of the long-wave radiation emitted by surrounding objects (terrestrial counterradiation) and by the sky (atmospheric counterradiation). The relative contributions of these two sources depend on the fractional parts they occupy in the field of view of the façade (50% each for a vertical facade and an unobstructed horizon, 100% atmospheric contribution for the surface of a flat roof, etc.). The terrestrial counterradiation is mainly a mixture of the Planckian long-wave emissions of different terrestrial surfaces whose emissivities will be close to 1 and whose temperatures at night will be close to the ambient air temperature.

The atmospheric counterradiation is a mixture of Planckian radiation emitted by cloud, fog, or haze droplets (if any) and non-Planckian radiation emitted by certain gaseous constituents of the atmosphere (mainly water vapor, carbon dioxide, and ozone). Instead of continuous Planckian spectra, these gas molecules emit band spectra and, thus, integrated over all wavelengths, less energy than a high-emissivity Planckian radiator at the same temperature. Since wavelengths that are strongly emitted are also strongly absorbed, the atmosphere is quite opaque to its own thermal emission so that almost all of the counterradiation arriving on the ground originates in the lowest 200 m of the atmosphere (assuming cloudless sky, a typical water vapor content for temperate latitudes, and the ground at sea level altitude). The temperature of this emitting air layer is usually not very different from the air temperature measured close to the ground (and, at night, not very different from the temperature of terrestrial objects). Despite this relatively small difference of temperatures, the clear sky emits noticeably less radiation than terrestrial objects due to the gaps in the discontinuous non-Planckian spectrum. Clouds will add some Planckian atmospheric radiation, depending on their size, thickness, and height (i.e., temperature). A thin high (cold) cirrus adds only up to 4% radiation; a thick and low (warm) stratus may increase the radiation by approximately 25% (Häckel 1999). For Central European climatic conditions and typical cloud cover, the average radiation intensity emitted by the sky is roughly 80% of the intensity emitted by terrestrial objects.

Since the façade of a building is such a terrestrial object, a net loss of thermal radiation will occur toward the sky, while the radiation exchange with other terrestrial objects will be roughly balanced. As a result, the long-wave radiation balance of the façade is usually negative, and at night (when no solar radiation can compensate the loss) its surface temperature may drop below the ambient air temperature until convective heat transport from the air toward the façade (plus any heat flow from indoors) counterbalances the radiative loss. If the cooled surface reaches the dew point of the ambient air, dew formation occurs. At normal ambient temperatures and for the usual nighttime relative humidities of 80% or more, the dew point is only 4 degrees or less below the air temperature. Dew formation is therefore common during the night, creates the problems mentioned above, and needs to be investigated further. For these and related purposes, WUFI® has been modified to explicitly account for the long-wave radiation exchange.

MODIFICATIONS IN WUFI

In previous versions of WUFI long-wave radiation, exchange of the facade with the surroundings was not explicitly accounted for. It was instead treated as an increase of the heat transfer coefficients: the default value of 17 W/m^{2}K for the exterior coefficient was assumed to include 6.5 W/m^{2}K of radiative and 10.5 W/m^{2}K of convective heat exchange, and similar assumptions were made for the interior coefficient. These numbers are based on measurements and can be considered as representative values for general energetic considerations (Schaube and Werner 1986). For most hygrothermal simulations, this simplified treatment is sufficient since assessment of the moisture balance in the construction usually does not require a perfectly detailed simulation of the thermal circumstances as long as the general temperature level is correctly reproduced. However, in the case of radiative cooling below the ambient air temperature ("overcooling"), the convective and the radiative heat fluxes at the exterior surface go in opposite directions and cannot be described by one single transfer coefficient any more.

While the treatment of the interior heat transfer coefficient remains unchanged, the value of the user-supplied exte-

rior heat transfer coefficient is now automatically reduced by 6.5 W/m^{2}K in order to isolate the purely convective portion of the coefficient (the user has the option to explicitly supply the convective coefficient, which is then not modified). For the outermost grid element (the façade surface) the equations built into WUFI contain a source term that allows the solar radiation to be treated as a heat source at the surface. In addition to solar radiation (read from the weather file and multiplied by the short-wave absorptivity) this source term has now been supplemented to include the terrestrial and atmospheric counterradiation (read from the weather file and multiplied by the long-wave emissivity of the surface) and—as a negative term—the thermal emission of the surface, as dependent on its temperature and its long-wave emissivity. The two counterradiation terms are reduced as appropriate to reflect their respective portions in the field of view of the surface, depending on its inclination. The atmospheric counterradiation reflected from the ground must not be neglected (see below).

As mentioned above, the emission is described by a nonlinear expression that contains the absolute temperature to the fourth power, whereas the numerics allow only linear source terms. The T^4 formula has therefore been linearized:

$$E = 5.67 \cdot 10^{-8} \cdot \varepsilon \cdot [(\vartheta_0 + 273{,}15)^4 + 4 \cdot (\vartheta_0 + 273{,}15)^3 \cdot (\vartheta - \vartheta_0)]$$

where ϑ_0 is a reference temperature (possible choices are the surface temperature from the previous time step or the surface temperature from the current internal iteration [6]) and ϑ is the as yet unknown surface temperature to be determined by the solution of the system of transport equations. Since the curvature of the T^4 curve is relatively small, the error caused by omitting the quadratic term is almost always less than 1% and usually much less.

SENSITIVITY

In thermal equilibrium by night, the small heat flow from indoors as well as latent heat from possible dew formation or evaporation are ignored. The net radiation loss is balanced by the convective heat gain. As a simplified example: if the combined counterradiation amounts to 300 W/m^2 and the surface emits 330 W/m^2, a convective flow of 30 W/m^2 toward the surface will result. Assuming a convective heat transfer coefficient of 10 W/m^{2}K, this corresponds to a surface temperature of 3 degrees below the ambient air temperature. An increase of 1% in the counterradiation (3 W/m^2) would change the net radiation flow (30 W/m^2) and, thus, the temperature difference (3 K) by 10%. Therefore, since the resulting temperature depends on the *difference* of two large numbers (radiative loss and gain), a small relative change in one of these numbers causes a large relative change in the net energy balance.

Particular care must therefore be taken to provide sufficiently accurate counterradiation data and emissivities and to allow for possible local peculiarities (for example, an obstructed horizon) if meaningful investigations of surface temperatures, dew formation statistics, etc., are intended. The following table illustrates the dependence of the results on slightly different input data. It shows to which extent the surface temperature falls below air temperature ("overcooling") for a north-facing 36-cm-thick monolithic brick wall with emissivity of 0.9, averaged over all temperature differences occurring at 4 a.m. in autumn nights (September through November), computed with the test reference year for Munich. Experience shows (see below) that such a massive wall should exhibit no or nearly no overcooling. In the first case, the reflection of atmospheric counterradiation by the ground was ignored and the original TRY was used. In the second case, the reflection was taken into account (assuming a reflectivity of $(1 - \varepsilon_{Earth}) = (1 - 0.9) = 10\%$), and the original TRY was used. In the third case, the reflection was taken into account and a modified TRY was used that should—at least roughly—allow for the local circumstances at a similar test wall in Holzkirchen: the ground temperature at night was assumed not to be identical to the air temperature but 2 K higher (based on ground temperatures measured in Holzkirchen), the emissivity of the ground was assumed to be 0.92 (grass) instead of 0.90, and the obstruction of the horizon by a nearby forest was allowed for. The terrestrial counterradiation in the file was thus on average increased by 14% and the atmospheric counterradiation reduced by 8%.

Input Variations	Nighttime Overcooling
No reflection, original TRY	–1.4 K
10% reflection, original TRY	–1.0 K
10% reflection, adapted TRY	–0.5 K

Obviously the effect of these variations is not negligible if the overcooling is to be investigated quantitatively, and some research will have to be spent on appropriate climatic data and the effect of local circumstances.

VALIDATION

A comparison of computed temperatures with analytical solutions is quite possible for the cases of steady-state and periodic boundary conditions (Heindel 1966). Currently, a strict comparison between computed and measured temperatures is not possible, since no simultaneously measured surface temperatures and counterradiation data are available for Holzkirchen or other locations (continuous counterradiation measurements at Holzkirchen are in preparation). Nevertheless, Figure 1 compares computed surface temperatures of a west-facing 24-cm-thick calcium silica brick wall with 8 cm ETICS (EIFS) of emissivity 0.9, exposed to the test reference year for Munich (adapted as described above) and measured (Holzkirchen, 1997-1999) surface temperatures of west-facing stucco samples whose surface temperatures have proved to be representative for complete walls with ETICS (EIFS) (Künzel and Sedbauer 2001). For each of the four seasons, the diurnal cycles have been averaged (i.e., averages have been computed for all temperatures at 0 h, for all temper-

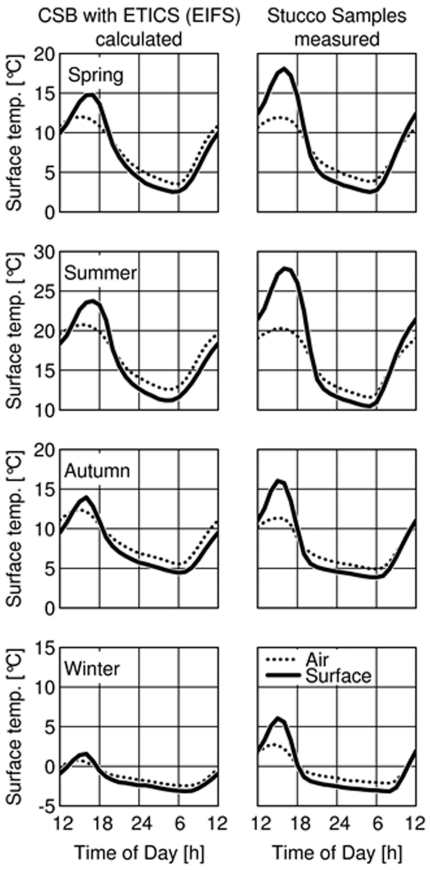

Figure 1 *Average diurnal surface temperature cycles for an ETICS (EIFS). Left, calculated with the adapted test reference year for Munich; right: measured at Holzkirchen (averages for 1997-1999).*

atures at 1 h, etc.) so that a representative diurnal cycle for the season results. Obviously, the average nightly overcooling can be reproduced very well by the calculation. No attempt has been made here to reproduce the daytime temperatures; the differences depend partly on different shortwave absorptivities of the calculated and measured walls and partly on different amounts of solar radiation during the measurements in Holzkirchen and in the TRY.

EXAMPLE CASE: CONDENSATION ON FAÇADES—INFLUENCE OF CONSTRUCTION TYPE AND ORIENTATION

As mentioned in Zillig (2003) suitable temperature and humidity conditions at the outer surfaces of walls are necessary for biological growth. For example, mold fungi need a relative humidity of 80% for a longer period of time (Sedlbauer 2001), and algae need a higher humidity for their growth or even liquid water, whereas an interim drying out does not harm them. Therefore, the periods of surface condensation and

Table 1. Variation of Different Surface Properties Used for Calculation of Surface Temperatures

Radiation Properties		
	Shortwave Radiation Absorption Coefficient	**IR-Emissivity**
Bright (standard)	0.4	0.9
Dark	0.6	0.9
Bright but low IR emissivity	0.4	0.6
Insulation layer thickness		
	Dimension	
Thick (standard)	10 cm	
Thin	5 cm	

the accumulated degree of cooling below dew-point temperature are taken as criteria to classify the results. In addition, the simulated surface temperatures will be compared with the dew-point temperature of the exterior air. The weather data are from the Fraunhofer-IBP weather station in Holzkirchen and the calculation period goes from 1 January to 25 September.

The following two typical construction assemblies with an almost identical U-factor of 0.35 Wm^2K^{-1} were investigated (from inside to outside):

- 20 cm concrete wall (heat conductivity 1.6 $Wm^{-1}K^{-1}$) with an ETICS respectively EIFS system (10 cm polystyrene slabs, heat conductivity 0.04 $Wm^{-1}K^{-1}$).
- 24 cm of aerated concrete (heat conductivity 0.1 $Wm^{-1}K^{-1}$).

Starting from these standard constructions, a series of simulations with varying parameters were performed to determine their influence on algae growth. First, the influence of orientation was worked out for both variants. As a second parameter, different surface properties were examined. In addition to the shortwave absorptivity, which mainly depends on the color of the rendering, the long-wave emissivity was tested. For ETICS (EIFS) the thickness of the insulation layer was varied, too. All variations are listed in Table 1.

Influence of the Orientation

For algae growth, spring and autumn are the most critical times in the year because in winter is mostly too cold and summer is mostly too hot and too dry. Figure 2 shows for the AAC wall with different orientations the simulated surface temperature during a sunny day. During the day the surface temperatures depend on irradiation and, therefore, the solar position. The north-facing wall gets no direct radiation but diffuse radiation from the sun. The temperature on the west-oriented wall never drops below the dew-point temperature. The reason is that the wall gets most sun radiation during the

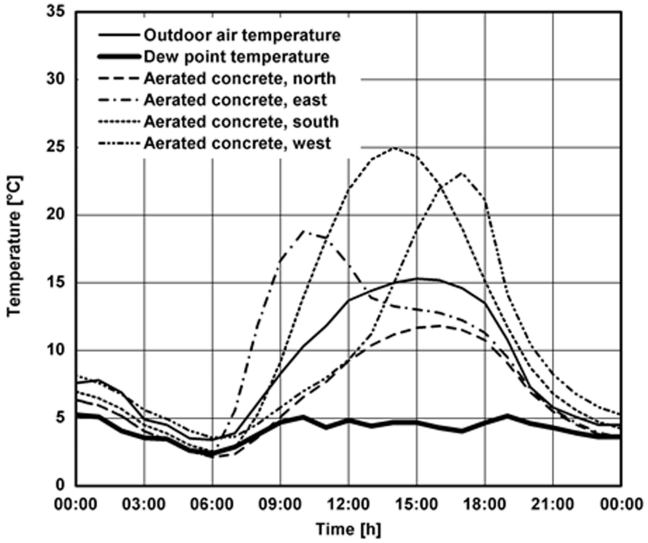

Figure 2 *Calculated surface temperatures depending on orientation during a sunny summer day (13 September) for a wall made out of aerated concrete. The outside air temperature and dew-point temperature are also shown.*

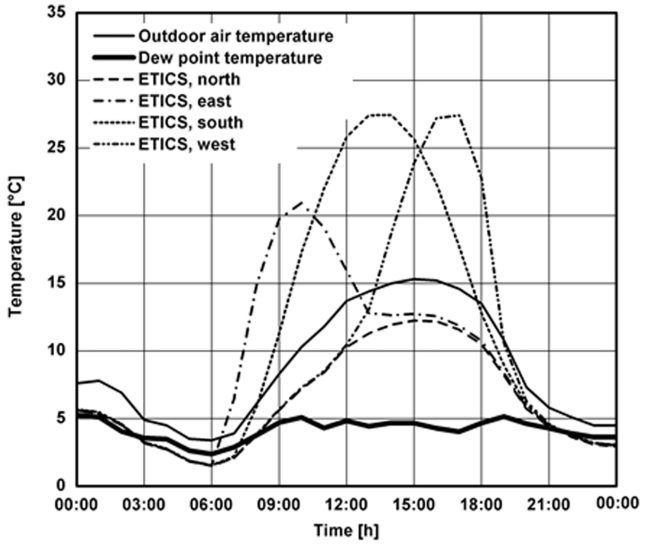

Figure 3 *Calculated surface temperatures depending on orientation during a sunny summer day (13 September) for a wall with ETICS. The outside air temperature and dew-point temperature are also shown.*

afternoon and the heat capacity keeps the wall "warm." The south-facing wall reaches dew-point temperature at about 3:00 in the morning, and at 8:00 the surface temperature drops shortly under dew-point temperature. At midnight the temperature on the east- and the north-oriented walls undershoots the dew-point temperature. While the east-facing wall warms up with the first sunlight at 6:00, the northern wall remains below dew point till 9:00.

The comparative courses for the wall with ETICS (EIFS) are shown in Figure 3. The major difference in the wall made of aerated concrete is that the thin plaster layer has a much smaller heat capacity. Therefore, the maximum temperatures are higher during the day. At night the total stored heat energy is less than in the AAC wall and is also emitted faster. The result is the undershooting of the dew-point temperature for eight to nine hours.

Figures 4 and 5 show the accumulated degree of cooling below dew point, which means for each hour at which the surface temperature is below dew-point temperature, the difference of surface and dew-point temperature is summarized. The figures shows an obvious difference between the two wall systems. For ETICS (EIFS) the accumulated degree of cooling below dew-point temperature is about twice as high as for the façade with aerated concrete. Some statistics about the hygrothermal behavior of the two different wall types are given in Table 2. Surprisingly, the west-facing wall made of aerated concrete has the shortest period of condensation. Referring to the accumulated degree of cooling below dew point, the western façade is only beaten by the northern one. The results for the wall with ETICS

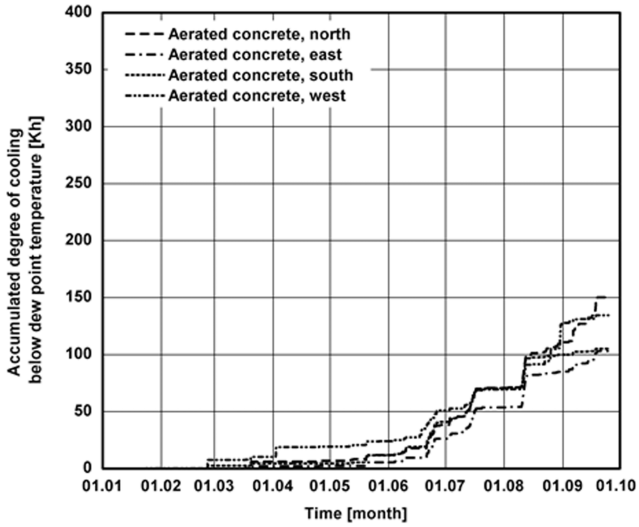

Figure 4 *Accumulated degree of cooling below dew-point temperature for walls made of aerated concrete with regard to orientation for the evaluation period (1 January-25 September).*

(EIFS) look a bit different. The west-facing wall has the longest duration of dew-point "undershooting" and the highest amount of condensation. The eastern wall shows the lowest risk of algal growth. For all orientations, the amount of condensation is obviously higher compared to the monolithic wall of aerated concrete.

Table 2. Calculated Periods of Surface Condensation Depending on Orientation for Walls Made of Aerated Concrete and Walls with ETICS for Evaluation Period

Direction	NORTH	EAST	SOUTH	WEST
Aerated concrete				
Periods of condensation (h)	369	302	298	282
Accumulated degree of cooling below dew-point temperature (Kh)	150	103	105	134
Medium daily period of condensation (h/d)	1.5	1.1	1.1	1.1
Average degree of cooling below dew-point temperature (K)	0.4	0.3	0.4	0.5
Wall with ETICS 10 cm				
Periods of condensation (h)	613	544	623	647
Amount of dew-point undershooting (Kh)	265	230	257	271
Daily dew-point undershooting (h/d)	2.3	2.0	2.3	2.4
Average degree of cooling below dew-point temperature (K)	0.4	0.4	0.4	0.4

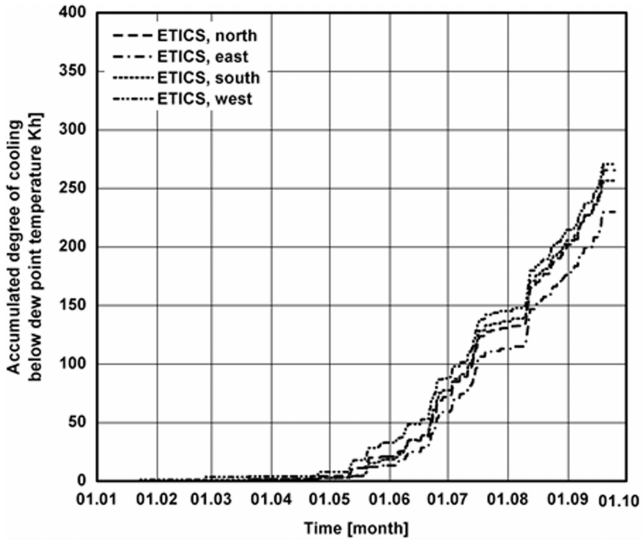

Figure 5 *Accumulated degree of cooling below dew-point temperature for walls with ETICS with regard to orientation for the evaluation period (1 January-25 September).*

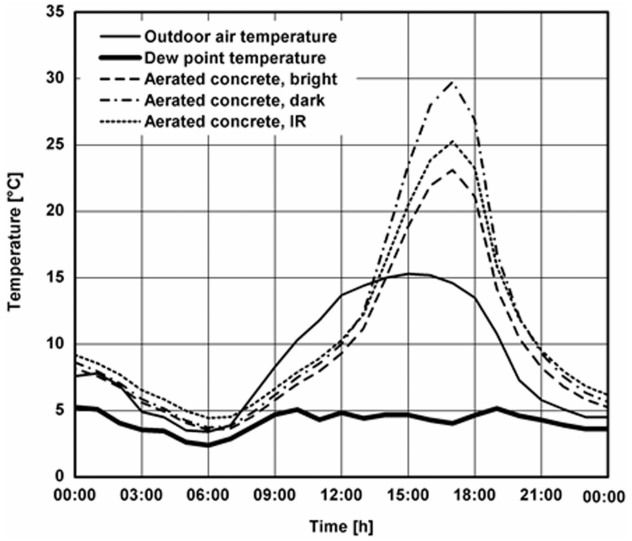

Figure 6 *Surface temperatures for west-facing walls made of aerated concrete with different surface properties. Data for a sunny summer day (13 September). The outdoor air temperature and dew-point temperature are also shown.*

Influence of the Color of the Plaster

As expected for both construction types, the maximum surface temperatures during the day are reached for those systems with a dark-colored plaster, as shown in Figure 6 and Figure 7. Interesting is the effect of the low IR emissivity. The simulated surface temperature of the wall systems with the bright plaster and low IR emissivity is higher than the standard case because every day the surface loses energy because of long-wave emission, and due to the lower emissivity of the surface, the maximum surface temperature is higher compared to the standard case. At night the thermal irradiation results in lower surface temperatures for the wall with ETICS (EIFS) in comparison to the aerated concrete wall. The surface temperatures of the systems with ETICS (EIFS) and standard bright or dark plaster even sink below the dew-point temperature. Only the systems with ETICS (EIFS) and low IR emissivity remain at the dew-point temperature. It is important to note that the surface temperatures of the wall made of aerated concrete remains mostly above dew-point temperature.

As can be seen in Figures 8 and 9, for both construction types the standard bright plaster shows the highest amount of surface condensation. It is followed by the dark plaster. The wall systems with low IR emissivity have the lowest amount. In the case of aerated concrete, the influence of color is considerably greater for the wall with ETICS (EIFS). The reason for this is the higher heat capacity. As shown in Figure 9, the comparatively good performance for ETICS (EIFS) with

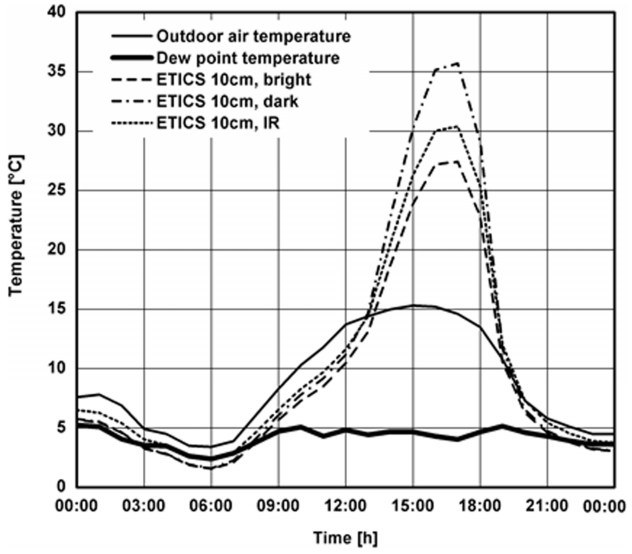

Figure 7 *Surface temperatures for west-facing walls with ETICS and different surface properties. Data for a sunny summer day (13 September). The outdoor air temperature and dew-point temperature are also shown.*

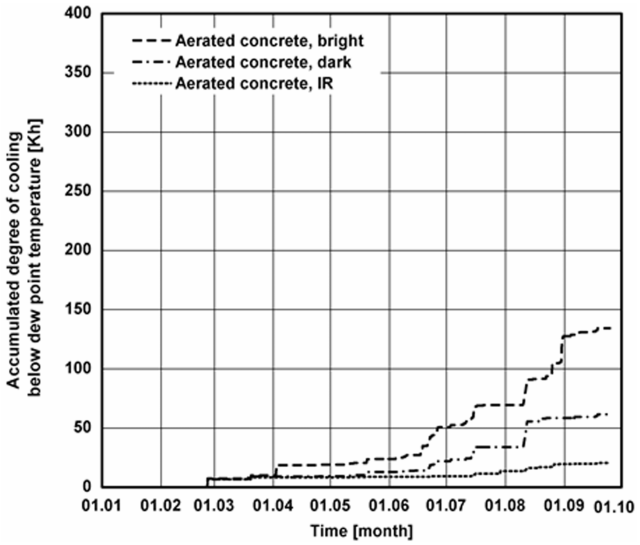

Figure 8 *Accumulated degree of cooling below dew-point temperature for walls made of aerated concrete depending on different surface properties for evaluation period (1 January-2 September).*

infrared active color shows one possibility to reduce the risk of algal growth on ETICS (EIFS). Table 3 lists some statistics of the effect of the above-mentioned surface properties.

Influence of ETICS (EIFS) Insulation Layer Thickness

As mentioned in Bagda (2002), the risk of algal growth on façades also depends on the thickness of the insulation layer. Therefore, additional calculations were carried out to demonstrate this effect. The standard case, an ETICS (EIFS) with 10 cm polystyrene, is compared with an ETICS (EIFS) with 5 cm polystyrene.

The higher thermal transmittance of the 5 cm system leads to a higher heat flow rate and, therefore, to higher surface temperatures of about 0.4 K during nighttime (Figure 10), but these higher surface temperatures are not sufficient to avoid surface condensation at all. As can be seen in Table 3, the "improvement" of reduced algal growth risk is not enough to lower these energy conservation measurements.

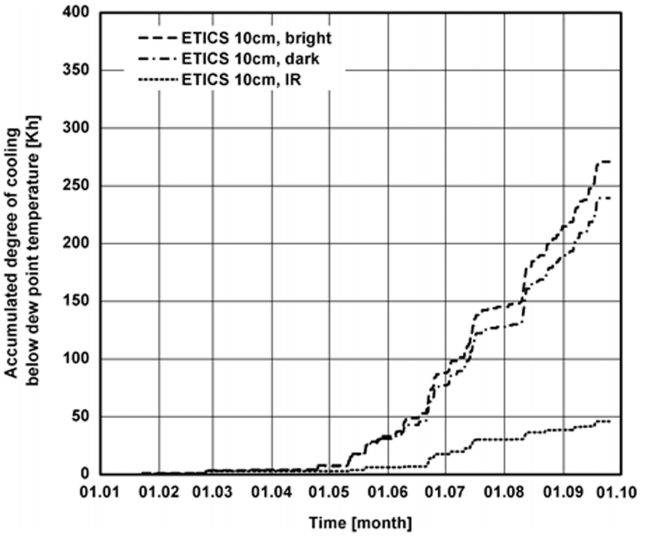

Figure 9 *Accumulated degree of cooling below dew-point temperature for walls with ETICS depending on different surface properties for evaluation period (1 January-25 September).*

OUTLOOK/CONCLUSION

The heat and moisture simulation program WUFI® has been modified to explicitly allow for the long-wave heat exchange between the surface of a façade and its surroundings. In particular, this allows quantitative calculation of nighttime overcooling due to long-wave emission, assessment of the resulting dew formation and biological growth conditions, as well as investigation of the effect of various countermeasures for different wall constructions. Preliminary validation shows good agreement with measurements but also demonstrates a strong sensitivity to variations in the boundary conditions.

The example case shows hygrothermal behavior of two different walls systems. As can also happen in real life, the east- and south-facing walls have the lowest risk of algal growth, north- and west-facing walls the highest one. In direct comparison of the wall made of aerated concrete with the wall with ETICS (EIFS), the advantage of monolithic walls is remarkable. Future research at the test side area in Holz-

Table 3. Periods of Surface Condensation of a West-Facing Wall Depending on the Construction Parameters and Different Surface Properties

Surface Property	Standard	Dark Plaster	With IR
Aerated concrete			
Periods of condensation (h)	282	176	84
Accumulated degree of cooling below dew-point temperature (Kh)	134	62	21
Medium daily period of condensation (h/d)	1.1	0.7	0.3
Average degree of cooling below dew-point temperature (K)	0.5	0.4	0.3
Wall with ETICS 10 cm, standard plaster			
Periods of condensation (h)	647	579	253
Accumulated degree of cooling below dew-point temperature (Kh)	271	239	46
Medium daily period of condensation (h/d)	2.4	2.2	1.0
Average degree of cooling below dew-point temperature (K)	0.4	0.4	0.2
Wall with ETICS 5 cm, standard plaster			
Periods of condensation (h)	519	468	124
Accumulated degree of cooling below dew-point temperature (Kh)	180	151	18
Medium daily period of condensation (h/d)	1.9	1.8	0.5
Average degree of cooling below dew-point temperature (K)	0.3	0.3	0.1

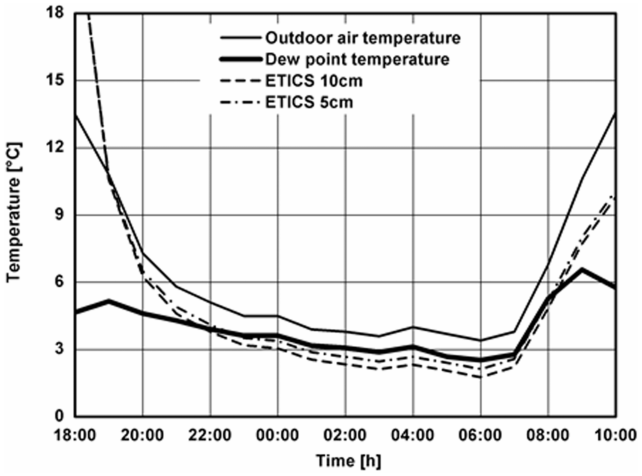

Figure 10 *Surface temperatures for west-facing walls with ETICS (EIFS) and different thicknesses of polystyrene layer during a clear night (1*3/14 S*eptember). The outdoor air temperature and dew-point temperature are also shown.*

kirchen will show if this behavior is reproducible. As surface temperatures are coupled with thermal transmittance of the construction, the thickness of the insulation has been varied, too, but the results show that even with 5 cm polystyrene, surface condensation occurs. The risk of algal growth is reduced, but at the expense of higher energy loss.

Only surface condensation has been investigated above, but the influence of driving rain as a humidity source has to be considered, too. Condensation occurs mainly in clear nights when irradiation has its maximum, and in these cloudless nights, rain is implausible. Especially in the area of Holzkirchen, west-facing walls get additional humidity from driving rain, but the main direction of driving rain is regionally different, and this effect has to be considered.

To assess the influence of driving rain on the risk of algal growth, the effects of hydrophilic or hydrophobic surfaces must be analyzed, too. To date the performance of highly hydrophobic surfaces, which leads to droplets on the surface, cannot be calculated correctly; therefore, this effect has to be examined separately in field tests. But there are more unsolved questions about environmental conditions needed for algal growth. In addition to dependence on the chemical composition of outer plaster or painting, the humidity and thermal conditions that support algal growth need to be examined. Further research is needed to get more information about the algal life on façades.

REFERENCES

Bagda, E. 2002. *Algen und Pilze (Algae and Fungi)*. Ausbau und Fassade, 4/2002: 42-43.

Häckel, H. 1999. *Meteorologie*. Ulmer, Stuttgart, 4. Aufl. 1999.

Heindl, W. 1966. Der Wärmeschutz einer ebenen Wand bei periodischen Wärmebelastungen. Die Ziegelindustrie, 18/1966, 685-693; 1/1967, 2-8; 18/1967, 593-599.

Hens, H. 1990. The hygrothermal behaviour of sloped roofs. *Proceedings Int. CIB W67 Symp. Rotterdam 1990,* Paper I 10.

Klinkenberg, G., and H. Venzmer. 2000. Algen auf Fassaden nachträglich wärmegedämmter Plattenbauten—Schadensmaß, Ursachen und Lösungen für ein Anti-Algenkonzept. FAS-Schriftenreihe Heft 11, S.29-40.

Künzel, H.M. 1995. *Simultaneous Heat and Moisture Transport in Building Components*. IRB Stuttgart, http://docserver.fhg.de/ibp/1995/kuenzel/001.pdf.

Künzel, H., and T. Großkinsky. 1989. Nicht belüftet, voll gedämmt: Die beste Lösung für das Steildach. wksb 34, H. 27, S. 1-7.

Künzel, H.M., and K. Sedlbauer. 2001. Biological growth on stucco. buildings. *Exterior Envelopes of Whole Buildings VIII*. Atlanta: American Society of Heating, Refrigerating and Air-Conditioning Engineers, Inc.

Leonhardt, H., and H. Sinnesbichler. 2000. Untersuchungen des langwelligen Wärmestrahlungsverhaltens von Fassadenanstrichen im Winter. IBP-Bericht RK-ES-05/2000.

Schaube, H., and H. Werner. 1986. Wärmeübergangskoeffizient unter natürlichen Klimabedingungen. IBP-Mitteilung 13, No. 109.

Sedlbauer, K. 2001. Prediction of mould growth on top of and inside building parts. Doctoral thesis, Stuttgart University, http://docserver.fhg.de/ibp/2001/sedlbauer/001.pdf.

Zillig, W., K. Lenz, K. Sedlbauer, and M. Krus. 2003. Condensation on the facade. Influence of construction type and orientation. *Proceedings of the 2nd International Conference on Building Physics, September 14-18, 2003, Antwerpen, Belgium*, pp. 437-444. J. Carmeliet, H. Hens, and G. Vermeir, eds.